Original Article

Eur J Breast Health 2025; 21(2): 93-105
DOI: 10.4274/ejbh.galenos.2025.2024-10-4

Breast Imaging: Correlation Between Axillary Lymph Nodes Apparent Diffusion Coefficient and Pathological Lymphovascular Invasion in Patients With Invasive Breast Cancer

Ahmad M. Mounir, Farah Ahmed Shokeir, Ghada H. Abd Elraouf

Department of Diagnostic Radiology, Mansoura University Faculty of Medicine, Mansoura, Egypt

ABSTRACT

Objective: Together with local invasion, one of the important characteristics of cancer is its capacity to spread, resulting in metastases. Before cancer cells metastasize to a secondary site, they must first enter and spread through the blood and lymph vasculature, this is known as lymphovascular invasion (LVI). This LVI and, to a much lesser extent, perineural and neural invasion are one of the biologic prerequisites for systemic spread and metastases. To evaluate the correlation between pre-operative apparent diffusion coefficient (ADC) of the ipsilateral enlarged axillary lymph nodes (LNs) and presence of LVI on post-operative pathology, in patients with invasive breast cancer.

Materials and Methods: This retrospective study was approved by the institutional review board. It included 100 female patients (mean age, 49 years; range, 30–68 years) with invasive breast cancer, who underwent preoperative magnetic resonance imaging (MRI) and breast surgery. On pre-operative MRI, the ADC was calculated for the ipsilateral enlarged axillary LN. Presence or absence of LVI was assessed on post-operative histopathology. Statistical analysis was performed to investigate any correlation between the ADC value of the axillary LNs and LVI in these patients.

Results: The mean ADC value of the ipsilateral enlarged axillary LNs was significantly lower in LVI positive cases compared to LVI negative cases (0.735×10^{-3} mm^2/s) *vs.* (1.024×10^{-3} mm^2/s), ($p<0.001$). Moreover, the mean Ki-67 in LVI positive cases was 46.12%, compared to 21.58% for LVI negative cases. This higher Ki-67 level in LVI positive cases indicates a greater degree of proliferation and thus the more aggressive nature of these tumors, and this was positively correlated with ADC values of the ipsilateral enlarged axillary LNs.

Conclusion: In cases of invasive breast cancer, the ADC value of the ipsilateral enlarged axillary LNs assessed on pre-operative MRI, and Ki-67 status of the tumor were significantly correlated to the LVI status on histopathological assessment. This ADC value may be useful as a predictor of axillary LN involvement, metastasis, and prognosis in invasive breast cancer.

Keywords: Invasive breast cancer; lymphovascular invasion; axillary lymph nodes; apparent diffusion coefficient; MRI

Cite this article as: Mounir AM, Shokeir FA, Elraouf GHA. Breast imaging: correlation between axillary lymph nodes apparent diffusion coefficient and pathological lymphovascular invasion in patients with invasive breast cancer. Eur J Breast Health.

Key Points

- Breast cancer is the most common cancer in women, with lymphovascular invasion detected in about 24.3% of cases, leading to higher metastasis and recurrence rates.
- Lymphovascular invasion is confirmed through histopathology, making it hard to detect preoperatively with standard imaging techniques.
- Diffusion-weighted imaging and the apparent diffusion coefficient can provide data on tumor cell density and aggressiveness, potentially predicting lymphovascular invasion presence.

Introduction

Breast cancer is the most common cancer in women, accounting for 30% of all new cancer cases and about 15% of total deaths in females, according to the latest cancer statistics in (1, 2) and is thus a serious threat to the health of women (3). Lymphovascular invasion (LVI) is defined as the presence of tumor emboli in lymphatic and vascular spaces within the area that surrounds an invasive carcinomas. LVI is detected in about 24.3% of patients with breast cancer (4). LVI is a key prognostic factor in cases of invasive breast cancer as patients with LVI positivity showed a higher rates of distant metastasis and also higher

Corresponding Author:
Ahmad M. Mounir MD; Ahmedmounir@mans.edu.eg

Received: 27.11.2024
Accepted: 02.03.2025
Epub: 13.03.2025

local recurrence rates after treatment (5). LVI is also associated with high Ki-67 levels. Ki-67 is an important immunohistochemical (IHC) marker used for evaluation of invasiveness, the proliferation activity, and prognosis in human tumors (6).

As LVI presence is confirmed histopathologically, based on a surgically excised specimen that contains the primary tumor and the peritumoral breast tissue, it is difficult to detect the presence of LVI by preoperative biopsy that contains the primary lesion only. So, preoperative multiplanar imaging with magnetic resonance imaging (MRI) of these cases may be expected to provide data that can predict the presence of LVI (7). Imaging modalities, such as ultrasound, computed tomography, and MRI, which is the most commonly used modality, cannot identify LVI accurately, because of various anatomical and morphological limitations of these modalities (8).

Diffusion-weighted imaging (DWI) is a specific functional MRI technique that evaluates the thermal motion of the water molecules within the tissue ultrastructure. The apparent diffusion coefficient (ADC) is a quantitative assessment parameter of DWI, which provides essential data about the density and aggressiveness of tumor cells (9, 10). Many earlier studies have discussed the role of the ADC in predicting LVI in invasive breast cancer patients with positive sentinel lymph nodes (LNs) (11).

The aim of the present study was to evaluate the correlation between pre-operative ADC of axillary LNs and the presence of LVI in post-operative histopathology in patients with invasive breast cancer. A further aim was to evaluate any correlation between Ki-67 and LVI.

Materials and Methods

This retrospective study included 100 female patients with single, unilateral, invasive breast cancer with positive ipsilateral axillary LNs, who underwent preoperative MRI and then breast surgery. Surgery was either conservative breast surgery or mastectomy, based on the size, and extension of the breast lesion, and axillary LN dissection was done in all the study patients. This study was done in the period from March 2023 to March 2024.

Ethics approval was approved and obtained by Mansoura Faculty of Medicine Institutional Research Board (approval number: R.24.04.2598, date: 18.05.2024). Informed consent was waived because this was a retrospective, anonymized study. Retrospective data were collected and analyzed from existing image archives.

Inclusion Criteria

Patients with unilateral, single, invasive breast cancer and with positive ipsilateral axillary LNs were included. Positive ipsilateral axillary LNs were confirmed clinically and radiologically. Invasive breast cancer patients, that is those with either invasive ductal or invasive lobular carcinoma, are characterized by the invasion of breast cancer cells into the basement membrane and spread from breast ducts or lobules to nearby breast tissue. By definition the breast cancer in these patients is no longer ductal carcinoma *in situ*, but has become an invasive type of breast cancer. The invasion and type of breast cancer also the Ki-67 level were determined on tru-cut needle biopsy from breast lesions which were performed in all patients before breast surgery or at the start of other types of therapy. Values for Ki-67 were evaluated by the histopathologist following recognized protocols for manual counting.

Criteria of molecular subtyping of breast cancer were:

1. Luminal subtype (subdivided into luminal A and luminal B)

Luminal A: human epidermal growth factor receptor 2 (HER2) negative [estrogen receptor (ER) positive, progesterone receptor (PR) negative/low, HER2 negative, Ki-67 proliferative index high]

Luminal B: HER2 positive (ER positive, PR positive or negative, HER2 positive, Ki-67 proliferative index varies)

2. Triple negative subtype (ER negative, PR negative, HER2 negative):

3. HER2 enriched (HER2 positive; ERBB2 positive): ER negative, PR negative, HER2/neu amplified or overexpressed.

The presence or absence of LVI was assessed on post-operative histopathological examination for all patients. These histopathological data were the "gold standard" to correlate the radiological data by.

Exclusion Criteria

Patients were excluded if they had bilateral breast cancer, as the aim was to assess LVI in breast cancer cases with ipsilateral enlarged axillary LNS, not with contralateral axillary LNs, and to correlate the pre-operative axillary LN ADC value with the post-operative LVI status of the breast lesion on the ipsilateral side. Patients were also excluded if they had unilateral breast cancer but there were multiple breast lesions, to ensure that the lesion evaluated on MRI was the same lesion assessed on post-operative pathology. Finally, patients were also excluded if they did not have pre-operative breast MRI or the diffusion study with an ADC map was not available.

MRI Technique

In all patients, MRI of the breast was performed using a 1.5 Tesla machine (Philips Ingenia, Best, The Netherlands). Examination of patients was performed in the prone position with the use of a dedicated 16-channel breast coil. DWI was obtained by a single shot spin echo sequence with the following parameters; (TR/TE/NEX): 5800/139 ms/1, b values used were 0, 500, and 1000 mm^2/sec. Diffusion gradients were sequentially applied in X, Y, and Z axes. Slice thickness was 4 mm, with 1 mm interslice gap, a 300-360 mm field of view, and matrix of (128x256). Total acquisition time was about 120 sec. Orthogonal diffusion images and ADC maps for all cases were performed.

Diffusion-Weighted Imaging Post-Processing

Four sets of DWI were obtained for each section. The first three sets of images (known as trace images), corresponding to sensitization gradients, were sequential applications in the three orthogonal planes. The ADC map (the last set), corresponding to the average diffusion images, where measurement of ADC for any region of interest (ROI) can be measured. The ADC maps were calculated by the MRI scanner in-built software.

Image Analyses

Conjoint interpretation of the MRI studies of the patients was done by three radiologists of 10, 10 and 12 years experience. The radiologists were blinded to patient pathological data. The ADC value was calculated for the most suspicious ipsilateral enlarged axillary LN. The ROIs were manually and carefully drawn along the solid area of the ipsilateral most suspicious LN and copied to the corresponding ADC maps, avoiding the areas with necrosis if present within the LN. No

less than three ROIs were used within the same ipsilateral enlarged LN, and then the mean ADC value for the lesion was calculated. ROI size was 20 mm^2.

Histopathological and Immunohistochemical Evaluation

Presence or absence of LVI was assessed on post-operative histopathological examination. These histopathological data were the gold standard to correlate the radiological data with.

Statistical Analysis

Data analysis was done by SPSS software, version 25 (IBM Inc., Armonk, NY, USA). Description of qualitative data was done using number and percentage. Quantitative data were described using mean ± standard deviation for data distributed normally after testing for normality using the Kolmogorov-Smirnov test. The obtained results significance was judged at the $p<0.05$ level.

If quantitative data was non-normal, the Mann-Whitney U test was used to compare between two studied groups while the Student t-test was used to compare two independent groups for normally distributed data. Receiver operating characteristics curve was used to calculate sensitivity and specificity of continuous variables with calculation of the optimal cut off point. Predictive values and accuracy were assessed using cross tabulation.

Results

This retrospective study included 100 female patients with a mean age of 49 years with a range of 30–68 years, with single unilateral invasive breast cancer and positive ipsilateral axillary LNs. Tumor data of the cases are shown in Table 1. Of the 100 patients, 61 had LVI on histopathological analysis and 39 did not.

Table 1. Laterality, number, and pathological types of the breast tumors in the studied cases

Patient data	*n*	%
Tumor laterality		
Unilateral	100	100
Bilateral	0	0
No. of the tumor in each study case	1	100
Pathological types of breast cancer in the studied patients		
Invasive duct carcinoma	93/100 cases	93%
Invasive lobular carcinoma	5/100 cases	5%
Mixed mucinous carcinoma	2/100 cases	2%

The mean ADC value of the ipsilateral enlarged axillary LNs was significantly lower in patients with LVI than in LVI negative cases with ADC values of 0.735×10^{-3} mm^2/s *vs.* 1.024×10^{-3} mm^2/s, respectively ($p<0.001$) (Table 2 and Figure 1).

In Figure 1, the mean Ki-67 in LVI positive cases was 46.12%, while this was 21.58% for LVI negative cases. This higher KI-67 level in LVI positive cases indicates a greater degree of proliferation and thus the more aggressive nature of these tumors, and this was positively correlated with ADC values of the ipsilateral enlarged axillary LNs.

In Table 3, the optimal cut-off point for ADC value in differentiating between LVI positive and negative cases was 0.889. Similarly, the cut off point for Ki-67 for differentiating between LVI positive and negative cases was 27.5% ($p<0.001$). The analysis showed relatively high sensitivity but only moderate specificity for ADC and Ki-67 when differentiating between LVI positive and negative cases, as shown in Table 3 and Figures 2 and 3.

Correlation between LVI and IHC parameters and MRI features of the tumors are shown in Table 4. There was a significant correlation between LVI and the number of infiltrated LNs. In LVI negative cases, all cases except for six (%) showed unaffected dissected LNs. In the six exceptions, each patient exhibited one infiltrated LN histopathologically. However, in LVI positive cases most patients had infiltrated dissected LNS, with a median of 4 infiltrated LNs per patient. However, once again there were six exceptions who had no infiltrated dissected LNs.

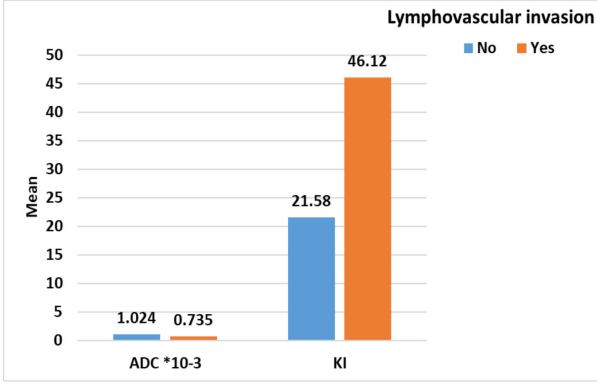

Figure 1. Mean ADC and Ki-67 % in differentiating between cases with and without LVI

LVI: Lymphovascular invasion; ADC: Apparent diffusion coefficient

Table 2. Comparison of mean ADC and Ki-67 in differentiating between cases with and without LVI

	Lymphovascular invasion		Test of significance
	Negative for LVI (*n* = 39)	Positive for LVI (*n* = 61)	
ADC x10^{-3}	1.024±0.22	0.735±0.17	*t* = 7.24 *p*<0.001*
Ki-67	21.58±13.15	46.12±22.59	*z* = 6.24 *p*<0.001*

t: Student t-test; z: Mann-Whitney U test; *: Statistically significant; LVI: Lymphovascular invasion; ADC: Apparent diffusion coefficient

In terms of IHC characteristics of the tumors, the luminal A molecular subtype was significantly correlated with negative LVI (28.2 %) *vs.* 8.2% for cases with positive LVI. However, luminal B molecular subtype was significantly correlated with positive LVI (65.6%) *vs.* 30.8% for negative LVI.

The number of infiltrated LNs was also significantly correlated with the ADC value of the axillary LNs, as shown in Table 5 and Figure 4. There was a significant negative correlation between this ADC value and the number of infiltrated LNs. The other IHC and MRI criteria of the tumors in the studied cases did not show significant correlation with the ADC value of the axillary LNS, with the exception of the having a non-circumscribed speculated margin which was significantly correlated with a lower ADC value (mean, 0.831±0.27), while circumscribed margin was significantly correlated with a higher ADC value (mean, 1.26±0.0), as shown in Table 6.

Discussion and Conclusion

Breast cancer is the most common cancer worldwide and the major cause of cancer related mortalities in women (12). Most breast cancer related mortalities are due primary tumor proliferation or due to distant metastasis (13). LVI is defined histopathologically as presence of tumor cells within the lymphatic or vascular spaces that encircles the primary carcinoma. Its positivity indicates a higher risk of cancer local recurrence or distant metastasis; so, its detection is important as a diagnostic or prognostic assessment of patients with breast cancer (14). Many studies have indicated the importance of the LVI in surgical intervention determination, providing guidance tool for neoadjuvant therapy evaluation, and suggesting optimal resection margins of the tumors (15, 16). However, identifying this LVI status accurately pre-operatively is a challenge, because it is identified accurately on histopatological examination following surgery.

Evaluation of LVI status in breast cancer patients, pre-operatively, may be done with the aid of some MRI morphological features, as the peritumoral edema, "adjacent vessel" sign, the DWI, and status of axillary LN on MRI (17-20). Dynamic MRI may play an important role in assessing LVI status, as it provides high quality multiplanar images and highly significant morphologic and functional data. It provides information on the volume, permeability, and the tumor vascular system angiogenesis (20, 21).

In our study we aimed to highlight the correlation between the ADC of the ipsilateral suspicious axillary LNs, and the LVI status in patients with invasive breast cancer.

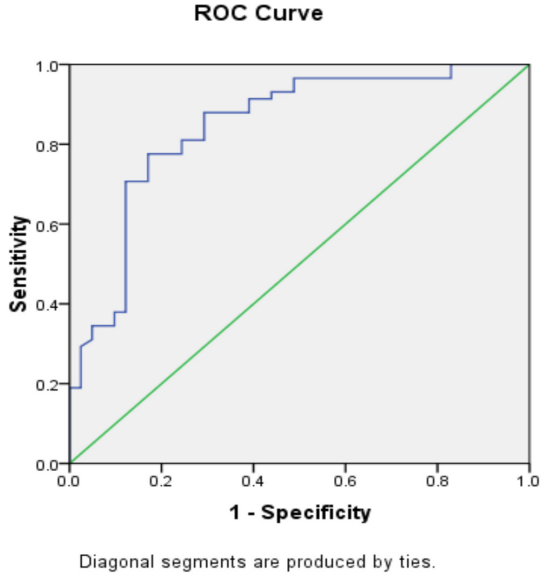

Figure 2. ROC curve of ADC in differentiating between cases with and without LVI

LVI: Lymphovascular invasion; ADC: Apparent diffusion coefficient; ROC: Receiver operating characteristics curve

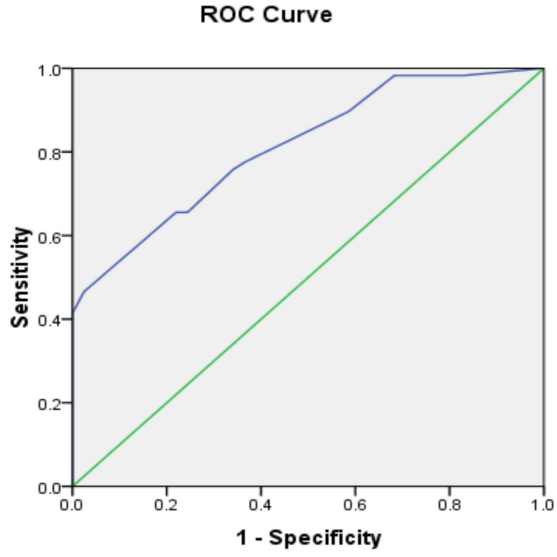

Figure 3. ROC curve of Ki-67 in differentiating between cases with and without LVI

LVI: Lymphovascular invasion; ADC: Apparent diffusion coefficient; ROC: Receiver operating characteristics curve

Table 3. Validity of ADC and Ki-67 in differentiating between cases with and without LVI

	AUC (95% CI)	*p*	Optimal cut-off	Sensitivity %	Specificity %	PPV%	NPV%	Accuracy %
ADCx10^{-3}	0.845 (0.764–0.926)	<0.001	0.889	87.9%	70.7%	81.0%	80.6%	80.1%
Ki-67	0.812 (0.731–0.893)	<0.001	27.5%	75.9%	65.9%	75.9%	65.9%	71.7%

PPV: Positive predictive value; NPV: Negative predictive value; AUC: Area under curve; LVI: Lymphovascular invasion; ADC: Apparent diffusion coefficient; CI: Confidence interval

Table 4. Correlation between lymphovascular invasion and clinicopathological features of the studied cases

	LVI		Test of significance	*p*
	No	**Yes**		
Number of infiltrated LNs Median (minimum-maximum)	0 (0–1)	4 (0–17)	$z = 7.61$	<0.001*
Tumor grade, *n* (%)				
I	3 (7.7)	2 (3.3)		
II	26 (66.7)	34 (55.7)	$\chi^2 = 3.0$	0.223
III	10 (25.6)	25 (41)		
ER score				
Median (minimum-maximum)	8 (0–8)	7 (0–8)	$z = 1.22$	0.223
PR score				
Median (minimum-maximum)	7 (0–8)	5 (0–8)	$z = 1.26$	0.209
HER2 status				
-VE	31 (79.5)	53 (86.9)	χ^2=0.969	0.325
+VE	8 (20.5)	8 (13.1)		
Molecular subtype				
Luminal A	11 (28.2)	5 (8.2)		
Luminal B	12 (30.8)	40 (65.6)	$\chi^2 = 13.12$	0.004*
HER-enriched	8 (20.5)	8 (13.1)		
Triple negative	8 (20.5)	8 (13.1)		
Amount of fibroglandular tissue (FGT)				
Entirely fatty	0	7 (11.5)		
Scattered FGT	15 (38.5)	30 (49.2)		
Heterogenous dense breast	18 (46.2)	19 (31.1)	$\chi^2 = 7.65$	0.054
Extremely dense breast	6 (15.4)	5 (8.2)		
BPE				
Minimal	0	7 (11.5)		
Mild	17 (43.6)	22 (36.1)	$\chi^2 = 4.91$	0.179
Moderate	19 (48.7)	28 (45.9)		
Marked	3 (7.7)	4 (6.6)		
Mass shape				
Irregular	33 (84.6)	52 (85.2)	$\chi^2 = 0.007$	0.931
Lobulated	6 (15.4)	9 (14.8)		
Mass margin				
Non-circumscribed speculated	18 (46.2)	32 (52.5)		
Non-circumscribed irregular	19 (48.7)	29 (47.5)	$\chi^2 = 3.32$	0.190
Circumscribed	2 (5.1)	0		
Mass internal enhancement pattern				
Heterogenous	35 (89.7)	50 (82)	$\chi^2 = 1.128$	0.288
RIM	4 (10.3)	11 (18)		
Kinetic curve type				
Pateau curve	8 (20.5)	9 (14.8)	$\chi^2 = 0.559$	0.455
Washout curve	31 (79.5)	52 (85.2)		

z: Mann-Whitney U test; χ^2: Chi-square test; *: Statistically significant; LVI: Lymphovascular invasion; HER2: Human epidermal growth factor receptor 2; ER: Estrogen receptor; PR: Progesterone receptor; BPE: Background parenchymal enhancement; LNs: Lymph nodes

Table 5. Correlation between ADC value and number of infiltrated LNs, ER & PR score

	ADC value	
	r	*p*-value
No of infiltrated LNs	-0.492	0.001*
ER score	-0.159	0.119
PR score	-0.104	0.301

r: Spearman correlation coefficient; LNs: Lymph nodes; ADC: Apparent diffusion coefficient; ER: Estrogen receptor; PR: Progesterone receptor

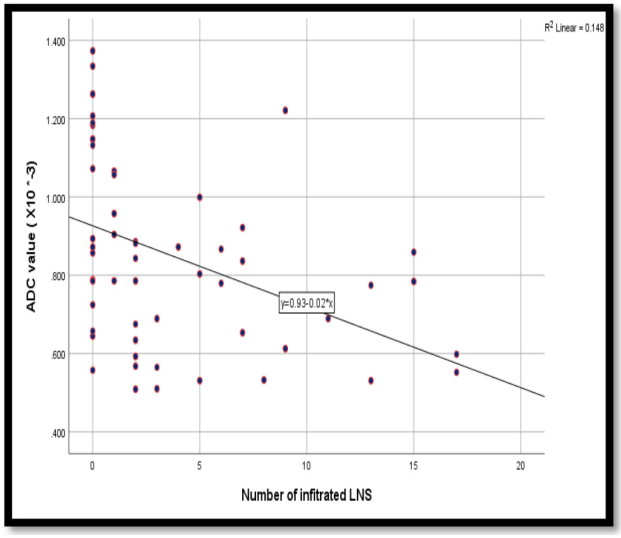

Figure 4. Scatter plot showing correlation between ADC & number of infiltrated LNs

ADC: Apparent diffusion coefficient; LNs: Lymph nodes

Markedly enlarged in size and abnormal LNs in morphology, especially when markedly different from other visible axillary LNs, are highly suggestive of nodal metastasis. Features of cortical thickening, loss of the fatty hilum, round shape or a (long-to-short axis ratio) of less than 2 are considered as typical morphologic criteria that can be seen with LNs metastasis (22). Also, according to Baltzer et al. (23), irregular margin, heterogenous cortex, perifocal edema which is seen as high T2 signal intensity in surrounding soft tissue, and asymmetry of the LNs in number or size compared with the contralateral side are findings suggestive of LN metastasis.

In our study, the mean ADC value of the ipsilateral enlarged axillary LNs was significantly lower in LVI positive than in LVI negative cases of invasive breast cancer (0.735×10^{-3} mm^2/s) *vs.* (1.024×10^{-3} mm^2/s), (p<0.001), with cut off point for ADC value in differentiating between LVI positive and negative cases was 0.889 as shown in Figures 5 and 6.

In our study, the mean Ki-67 in LVI positive cases was 46.12%, while was 21.58% for LVI negative cases. The cut-off point for Ki-67 in differentiating between LVI positive and negative cases was 27.5 (p-value less than 0.001). This higher Ki-67 level in LVI positive cases reflected the more aggressive nature of these tumors and their higher proliferation activity, and this correlated positively with ADC values of the ipsilateral enlarged axillary LNs as shown in Figures 7 and 8.

This is consistent with the results of Liu et al. (24), study in which the LVI positive group had higher Ki-67 expression level (>30%) than the LVI negative group and the difference was statistically significant (p = 0.012).

Also agreed with results of literatures which confirmed that higher KI-67 is associated with higher tumor grade, LVI, metastasis, and recurrence rate (25-27).

Our results agreed with the results of Klingen et al. (28) who reported that LVI was associated with some features of aggressive breast cancer as LN positive tumors and higher Ki-67 expression.

Also our results were in line with a review that has shown that the presence of LVI correlates with locoregional LN involvement (29).

Also, our study results agreed with results of Zhang et al. (30), retrospective study, who found a strong association between the LN status and the LVI status.

In Yang et al. (31), study they found correlation between LN criteria including larger size, and presence of necrosis, with the LVI status. But, they didn't include the ADC value of the axillary LN on the LN status data. Also, they found a border line correlation of the Ki-67 level with the LVI status.

Some studies recently, have shown that ADC value may be a good prognostic factor correlated to aggressiveness of tumors in breast cancer patients (32-34). Other current retrospective cohort studies concluded that ADC values of breast tumors were lesser in the LVI positive groups than the negative ones (11, 35). Lower ADC value is related to decrease in osmosis speed within tumor tissues and to higher proliferation rates of tumor cells. LVI was significantly concomitant to a higher cell proliferation level of the tumor (high Ki-67 level) (11).

Our results agreed with results of Byon et al. (36) , retrospective study that included 435 cases of breast cancer which compared "standard lower axillae" and "combined entire axilla" MRI protocols, they determined that axillae positivity (odds ratio: 5.9) and positive peritumoral edema (odds ratio: 12.3) at the standard protocol of MRI were predictive factors of high level axillary LNs metastasis, and with exclusion of axillary findings, peritumoral edema or mutifocality and multicentricity were predictive factor of high level axillary LNs metastasis, also, the LVI and the peritumoral edema were prognostic factors of advanced axillary LNs metastasis.

Our results agreed with Chen et al. (37), who found that the LVI in axillary LN metastasis group was significantly higher than that in non -axillary LN metastasis group (37.50% *vs.* 6.10%, $p<0.001$). And their logistic regression analysis suggested that LVI was one of the risk factors for axillary LN metastasis in patients with invasive breast cancer.

Our results showed relatively high sensitivity and moderate specificity for ADC and Ki-67 in differentiating between LVI positive and negative cases (87.9% sensitivity, 70.7% specificity) for ADC and (75.9% sensitivity, 65.9%) for Ki-67, with (81.0% PPV, 80.6% NPV, 80.1% accuracy) for ADC, and (85.9% PPV, 75.9% NPV, 71.7% accuracy) for Ki-67.

Table 6. Relationship between ADC value and clinicopathological features

	ADC value	Test of significance	*p*
	Mean ± standard deviation		
Tumor grade			
I	0.825±0.25		
II	0.838±0.26	F = 0.604	0.549
III	0.893±0.21		
HER2 status			
-VE	0.855±0.25	*t* = 0.124	0.902
+VE	0.864±0.16		
Molecular subtype			
Luminal A	0.849±0.23		
Luminal B	0.853±0.26	F = 0.028	0.994
HER-enriched	0.864±0.16		
Triple negative	0.869±0.24		
Amount of fibroglandular tissue			
Entirely fatty	0.847±0.15		
Scattered fibroglandular tissue	0.784±0.23	F = 3.17	0.028
Heterogenous dense breast	0.928±0.25		
Extremely dense breast	0.940±0.17		
BPE			
Minimal	0.787±0.19		
Mild	0.827±0.22	F = 0.931	0.429
Moderate	0.876±0.26		
Marked	0.959±0.17		
Mass shape			
Irregular	0.843±0.24	*t* = 1.35	0.180
Lobulated	0.934±0.23		
Mass margin			
Non-circumscribed speculated	0.831±0.27		
Non-circumscribed irregular	0.867±0.19	F = 3.34	0.039*
Circumscribed	1.26±0.0		
Mass internal enhancement pattern			
Heterogenous	0.867±0.24	*t* = 1.05	0.298
RIM	0.797±0.16		
Kinetic curve type			
Pateau curve	0.909±0.16	*t* = 0.997	0.321
Washout curve	0.845±0.252		

F: One-Way ANOVA test; t: Student t-test; HER2: Human epidermal growth factor receptor 2; ER: Estrogen receptor; PR: Progesterone receptor; BPE: Background parenchymal enhancement

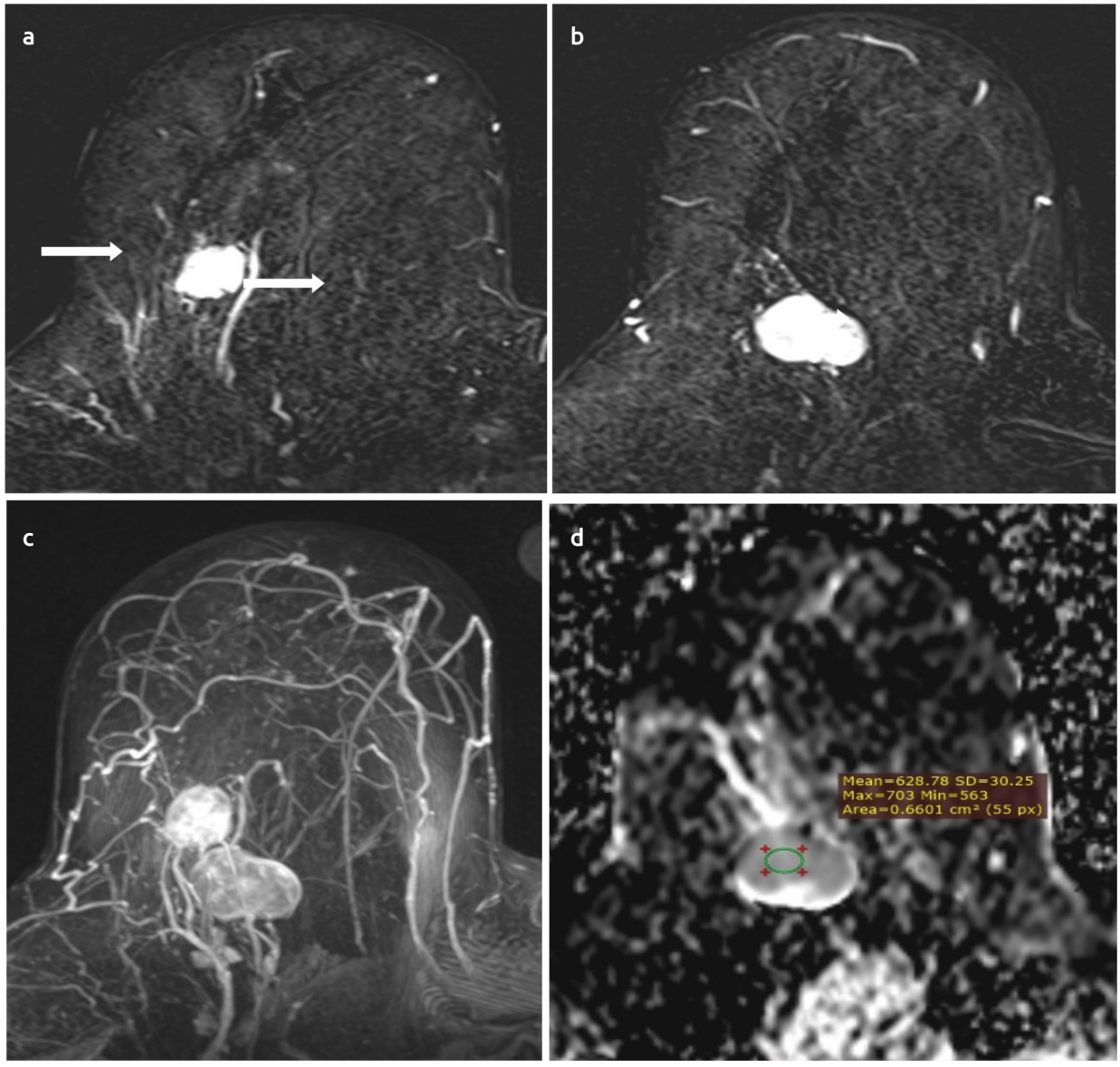

Figure 5. Fifty-five years old female with luminal B right breast cancer. Post-operative pathology revealed: High grade infiltrating duct carcinoma with low grade DCIS component (5%), with detected lymphovascular emboli, no perineural invasion. Examination of Ki-67 stained slide revealed nuclear staining in 30% of tumor cells. a. Post contrast subtraction MRI image showing malignant looking irregular mass in right breast (white arrow). b. Post contrast MRI subtraction image showing ipsilateral enlarged axillary tail suspicious LN (white arrow). c. Subtraction MIP image showing the mass and the LN. d. Mean ADC value of this LN was $0.628x10^{-3}$ mm^2/s

LNs: Lymph nodes; ADC: Apparent diffusion coefficient; MRI: Magnetic resonance imaging; DCIS: Ductal carcinoma in situ; MIP: Maximum intensity projection

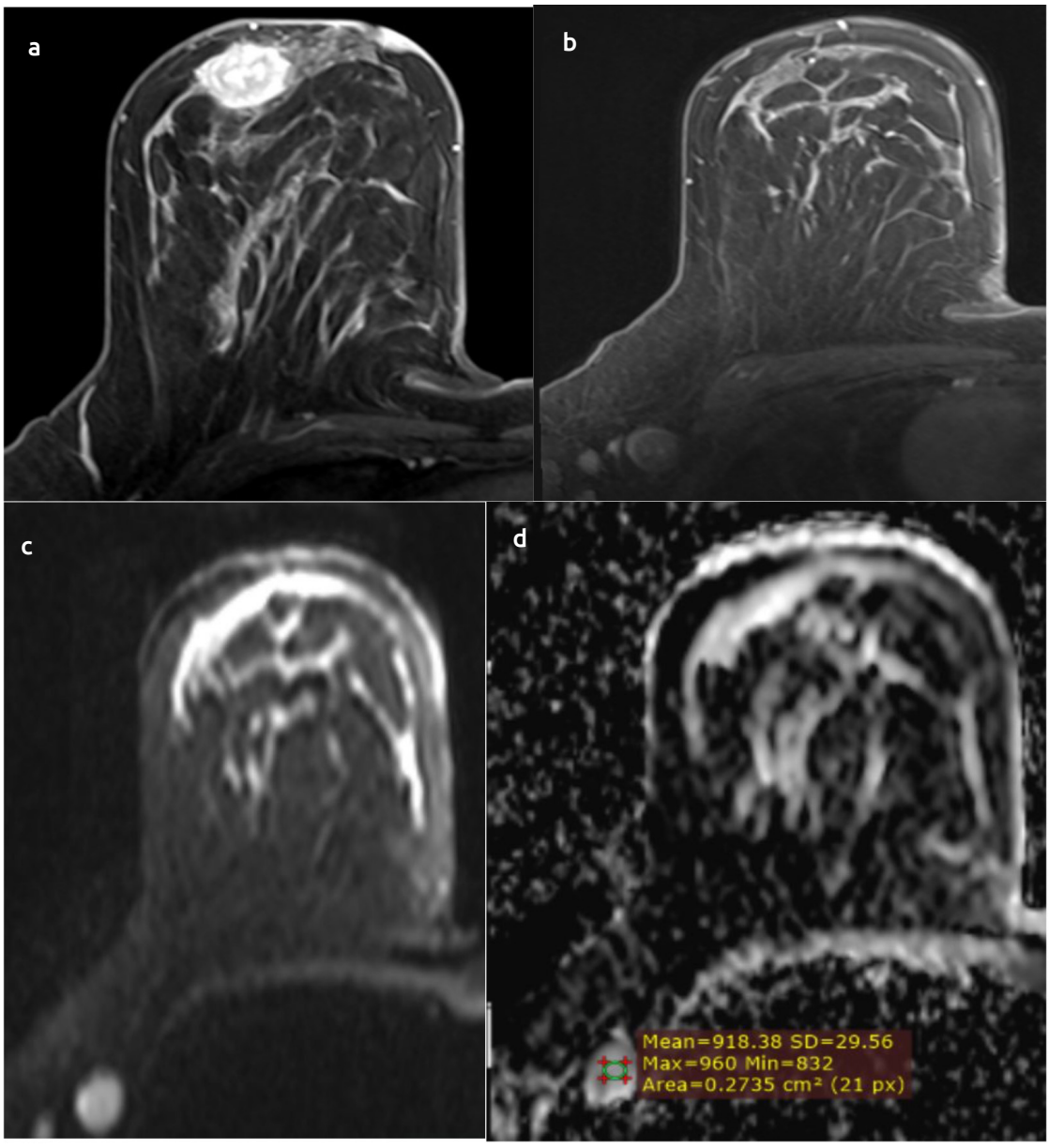

Figure 6. Thirty-two years old female with luminal B right breast cancer. Post-operative pathology revealed: Grade II invasive duct carcinoma associated with high grade ductal carcinoma *in situ* about 5%. No lymphovascular invasion or perineural spread. Ki-67: Positive nuclear reaction in about (20) % of tumor cells. a. Post contrast subtraction MRI image showing malignant looking irregular mass in right breast b. Post contrast MRI subtraction image showing ipsilateral enlarged suspicious axillary LN (white arrow). c. Diffusion image showing high SI of the LN. d. ADC map showing low SI and restricted diffusion of the LN. Mean ADC value of this LN was 0.905 $x10^{-3}$ mm^2/s

LNs: Lymph nodes; ADC: Apparent diffusion coefficient; MRI: Magnetic resonance imaging; SI: Sacroiliac

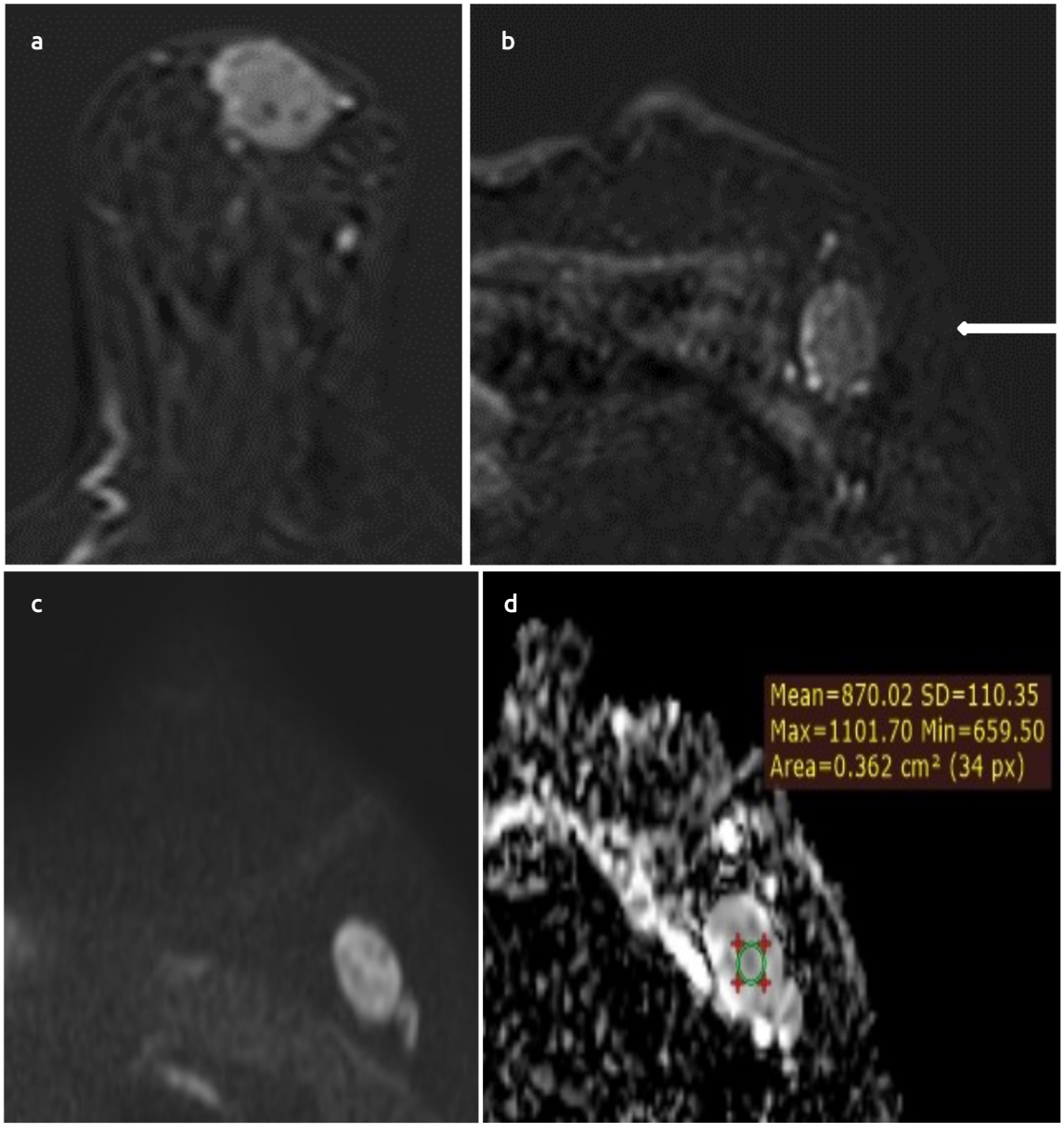

Figure 7. Forty-one years old female patient with triple negative left breast cancer. Post-operative pathology revealed grade III invasive duct carcinoma, with negative lymphvascular invasion. Ki-67 was about 70%, high proliferation index. a. Subtraction post contrast image showing left retroareolar suspicious mass. b. Subtraction post contrast image showing enhanced suspicious left axillary LN (white arrow). c. Diffusion image showing high SI of the LN in diffusion image. d. ADC map showing mean ADC value of the axillary LN of 0.870 x10^{-3} mm^2/s

LNs: Lymph nodes; ADC: Apparent diffusion coefficient

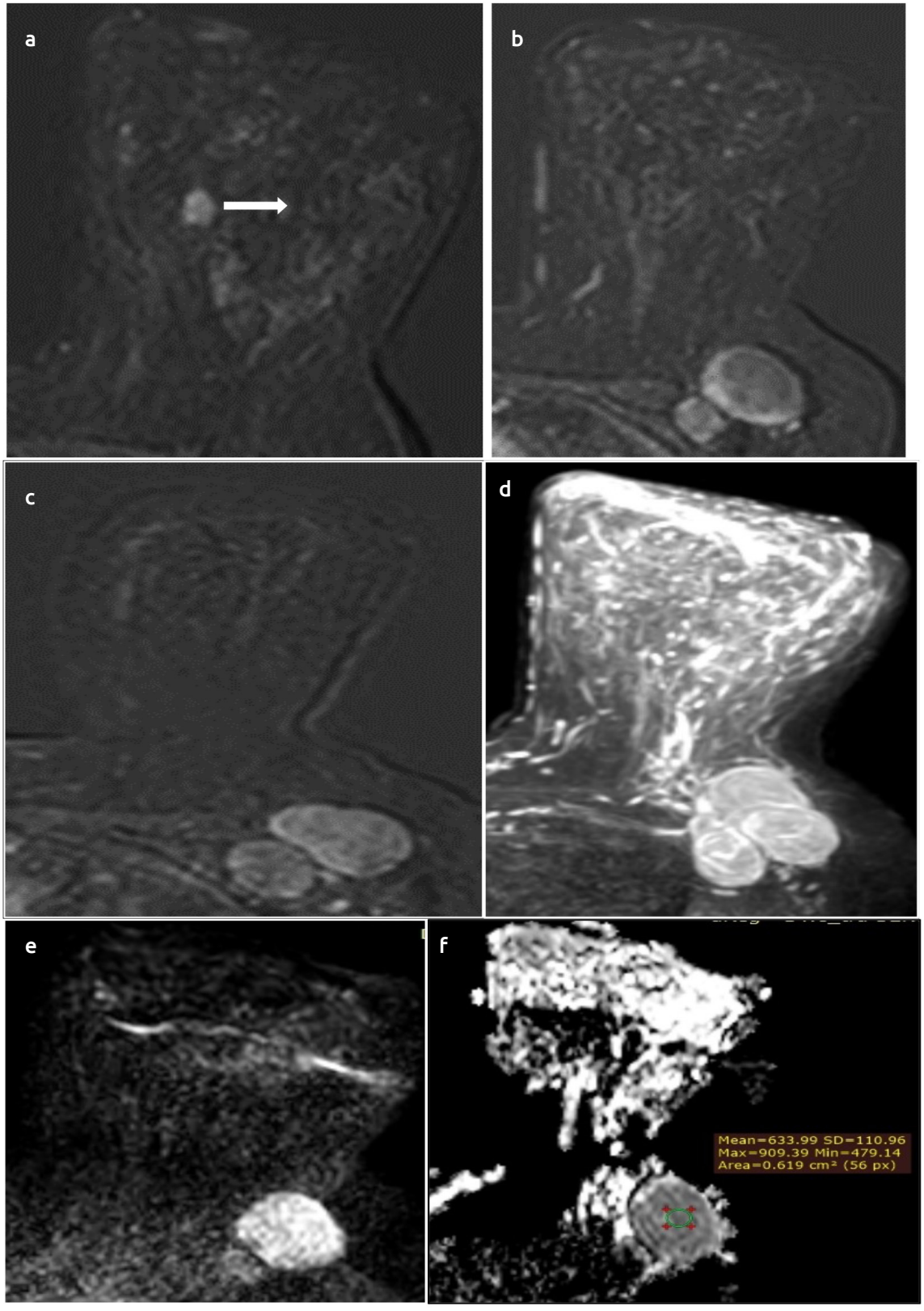

Figure 8. Forty-nine years old female patient with triple negative left breast cancer. Post-operative pathology revealed grade II invasive duct carcinoma with scattered foci of high-grade ductal carcinoma *in situ*, with positive lymphvascular invasion and perineural spread. Ki-67 was about 80%, high proliferation index. a. Subtraction post contrast image showing small suspicious mass in left breast (arrow). b, c. Subtraction post contrast images showing enhanced suspicious left axillary LNs. d. subtraction MIP images showing the left axillary LNs. e. Diffusion image showing high SI of the left axillary LN. f. ADC map showing ADC value of the largest suspicious left axillary LN of 0.633 $x10^{-3}$ mm^2/s

LNs: Lymph nodes; ADC: Apparent diffusion coefficient; SI: Sacroiliac; MIP: Maximum intensity projection

Our results are consistent with the overall sensitivity, specificity in predicting LVI of Kayadibi et al. (38), study who used machine learning and radiomics based on 3D segmentation of ADC maps can be used to predict LVI status in breast cancer in their study, the area under the curve and accuracy were 0.726 and 63.5% in the training data respectively, and (0.732 and 76.7%) in the test data, respectively. Overall sensitivity and positive predictive values were 68% and 69.6% in the training data, and 84.6% and 78.6% respectively in the test data in their study.

We concluded that the ADC value of the ipsilateral enlarged axillary LNs, and Ki-67 status of the tumor were highly correlated to the status of LVI in cases of invasive breast cancer. So, may be used as a tool for prediction of the axillary LN involvement, metastasis, and prognosis of the patients with invasive breast cancer.

Ethics

Ethics Committee Approval: Ethics approval was approved and obtained by Mansoura Faculty of Medicine Institutional Research Board (approval number: R.24.04.2598, date: 18.05.2024).

Informed Consent: Informed consent was waived because this was a retrospective, anonymized study.

Footnotes

Authorship Contributions

Surgical and Medical Practices: F.A.S., G.H.A.E.; Concept: A.M.M.; Design: A.M.M., F.A.S.; Data Collection or Processing: A.M.M., G.H.A.E.; Analysis or Interpretation: A.M.M., F.A.S., G.H.A.E.; Literature Search: A.M.M., G.H.A.E.; Writing: A.M.M., G.H.A.E.

Conflict of Interest: No conflict of interest was declared by the authors.

Financial Disclosure: The authors declared that this study received no financial support.

References

1. Mohammed RA, Martin SG, Mahmmod AM, Macmillan RD, Green AR, Paish EC, et al. Objective assessment of lymphatic and blood vascular invasion in lymph node-negative breast carcinoma: findings from a large case series with long-term follow-up. J Pathol. 2011; 223: 358-365. (PMID: 21171081). [Crossref]
2. Torous VF, Simpson RW, Balani JP, Baras AS, Berman MA, Birdsong GG, et al. College of American Pathologists cancer protocols: from optimizing cancer patient care to facilitating interoperable reporting and downstream data use. JCO Clin Cancer Inform. 2021; 5: 47-55. (PMID: 33439728) [Crossref]
3. Siegel RL, Miller KD, Fuchs HE, Jemal A. Cancer statistics, 2021. CA Cancer J Clin. 2021; 71: 7-33. doi: 10.3322/caac.21654. Erratum in: CA Cancer J Clin. 2021; 71: 359. (PMID: 33433946) [Crossref]
4. Houvenaeghel G, Cohen M, Classe JM, Reyal F, Mazouni C, Chopin N, et al. Lymphovascular invasion has a significant prognostic impact in patients with early breast cancer, results from a large, national, multicenter, retrospective cohort study. ESMO Open. 2021; 6: 100316. (PMID: 34864349) [Crossref]
5. Chernofsky MR, Felix JC, Muderspach LI, Morrow CP, Ye W, Groshen SG, et al. Influence of quantity of lymph vascular space invasion on time to recurrence in women with early-stage squamous cancer of the cervix. Gynecol Oncol. 2006; 100: 288-293. (PMID: 16182347) [Crossref]
6. Fusco A, Zatelli MC, Bianchi A, Cimino V, Tilaro L, Veltri F, et al. Prognostic significance of the Ki-67 labeling index in growth hormone-secreting pituitary adenomas. J Clin Endocrinol Metab. 2008; 93: 2746-27450. (PMID: 18460561) [Crossref]
7. Igarashi T, Furube H, Ashida H, Ojiri H. Breast MRI for prediction of lymphovascular invasion in breast cancer patients with clinically negative axillary lymph nodes. Eur J Radiol. 2018; 107: 111-118. (PMID: 30292254) [Crossref]
8. Patel S, Liyanage SH, Sahdev A, Rockall AG, Reznek RH. Imaging of endometrial and cervical cancer. Insights Imaging. 2010; 1: 309-328. (PMID: 22347925) [Crossref]
9. Sun Y, Tong T, Cai S, Bi R, Xin C, Gu Y. Apparent diffusion coefficient (ADC) value: a potential imaging biomarker that reflects the biological features of rectal cancer. PLoS One. 2014; 9: e109371. (PMID: 25303288) [Crossref]
10. Thoeny HC, Forstner R, De Keyzer F. Genitourinary applications of diffusion-weighted MR imaging in the pelvis. Radiology. 2012; 263: 326-342. (PMID: 22517953) [Crossref]
11. Mori N, Mugikura S, Takasawa C, Miyashita M, Shimauchi A, Ota H, et al S. Peritumoral apparent diffusion coefficients for prediction of lymphovascular invasion in clinically node-negative invasive breast cancer. Eur Radiol. 2016; 26: 331-339. Erratum in: Eur Radiol. 2016; 26: 340-341. (PMID: 26024846) [Crossref]
12. Sung H, Ferlay J, Siegel RL, Laversanne M, Soerjomataram I, Jemal A, et al. Global Cancer Statistics 2020: GLOBOCAN estimates of incidence and mortality worldwide for 36 cancers in 185 countries. CA Cancer J Clin. 2021; 71: 209-249. (PMID: 33538338) [Crossref]
13. Waks AG, Winer EP. Breast cancer treatment: a review. JAMA. 2019; 321: 288-300. (PMID: 30667505) [Crossref]
14. Britto AV, Schenka AA, Moraes-Schenka NG, Alvarenga M, Shinzato JY, Vassallo J, et al. Immunostaining with D2-40 improves evaluation of lymphovascular invasion, but may not predict sentinel lymph node status in early breast cancer. BMC Cancer. 2009; 9: 109. (PMID: 19356249) [Crossref]
15. Zhong YM, Tong F, Shen J. Lympho-vascular invasion impacts the prognosis in breast-conserving surgery: a systematic review and meta-analysis. BMC Cancer. 2022; 22: 102. (PMID: 35073848) [Crossref]
16. Rezaianzadeh A, Talei A, Rajaeefard A, Hasanzadeh J, Tabatabai H, Tahmasebi S, et al. Vascular invasion as an independent prognostic factor in lymph node negative invasive breast cancer. Asian Pac J Cancer Prev. 2012; 13: 5767-5772. (PMID: 23317254) [Crossref]
17. Cheon H, Kim HJ, Lee SM, Cho SH, Shin KM, Kim GC, et al. Preoperative MRI features associated with lymphovascular invasion in node-negative invasive breast cancer: A propensity-matched analysis. J Magn Reson Imaging. 2017; 46: 1037-1044. (PMID: 28370761) [Crossref]
18. Uematsu T. Focal breast edema associated with malignancy on T2-weighted images of breast MRI: peritumoral edema, prepectoral edema, and subcutaneous edema. Breast Cancer. 2015; 22: 66-70. (PMID: 25336185) [Crossref]
19. Cheon H, Kim HJ, Kim TH, Ryeom HK, Lee J, Kim GC, et al. Invasive breast cancer: prognostic value of peritumoral edema identified at preoperative MR imaging. Radiology. 2018; 287: 68-75. (PMID: 29315062) [Crossref]
20. Choi BB. Dynamic contrast enhanced-MRI and diffusion-weighted image as predictors of lymphovascular invasion in node-negative invasive breast cancer. World J Surg Oncol. 2021; 19: 76. (PMID: 33722246) [Crossref]
21. Song D, Yang F, Zhang Y, Guo Y, Qu Y, Zhang X, et al. Dynamic contrast-enhanced MRI radiomics nomogram for predicting axillary lymph node metastasis in breast cancer. Cancer Imaging. 2022; 22: 17. (PMID: 35379339) [Crossref]

22. Ecanow JS, Abe H, Newstead GM, Ecanow DB, Jeske JM. Axillary staging of breast cancer: what the radiologist should know. Radiographics. 2013; 33: 1589-612. (PMID: 24108553) **[Crossref]**
23. Baltzer PA, Dietzel M, Burmeister HP, Zoubi R, Gajda M, Camara O, et al. Application of MR mammography beyond local staging: is there a potential to accurately assess axillary lymph nodes? evaluation of an extended protocol in an initial prospective study. AJR Am J Roentgenol. 2011; 196: W641-7. (PMID: 21512057) **[Crossref]**
24. Liu Z, Li R, Liang K, Chen J, Chen X, Li X, et al. Value of digital mammography in predicting lymphovascular invasion of breast cancer. BMC Cancer. 2020; 20: 274. (PMID: 32245448) **[Crossref]**
25. Menon SS, Guruvayoorappan C, Sakthivel KM, Rasmi RR. Ki-67 protein as a tumour proliferation marker. Clin Chim Acta. 2019; 491: 39-45. (PMID: 30653951) **[Crossref]**
26. Altundag K. Larger tumor size detected by sonography might not always reflect increased risk of axillary lymph node metastasis in patients with breast cancer. J Ultrasound Med. 2019; 38: 2521. (PMID: 30637782) **[Crossref]**
27. Peng JH, Zhang X, Song JL, Ran L, Luo R, Li HY, et al. Neoadjuvant chemotherapy reduces the expression rates of ER, PR, HER2, Ki67, and P53 of invasive ductal carcinoma. Medicine (Baltimore). 2019; 98: e13554. Erratum in: Medicine (Baltimore). 2022; 101: e28714. (PMID: 30633152) **[Crossref]**
28. Klingen TA, Chen Y, Stefansson IM, Knutsvik G, Collett K, Abrahamsen AL, et al. Tumour cell invasion into blood vessels is significantly related to breast cancer subtypes and decreased survival. J Clin Pathol. 2017; 70: 313-319. (PMID: 2761250) **[Crossref]**
29. Rampaul RS, Pinder SE, Elston CW, Ellis IO; Nottingham Breast Team. Prognostic and predictive factors in primary breast cancer and their role in patient management: The Nottingham Breast Team. Eur J Surg Oncol. 2001; 27: 229-238. (PMID: 11373098) **[Crossref]**
30. Zhang C, Liang Z, Feng Y, Xiong Y, Manwa C, Zhou Q. Risk factors for lymphovascular invasion in invasive ductal carcinoma based on clinical and preoperative breast MRI features: a retrospective study. Acad Radiol. 2023; 30: 1620-1627. (PMID: 36414494) **[Crossref]**
31. Yang X, Fan X, Lin S, Zhou Y, Liu H, Wang X, et al. Assessment of lymphovascular invasion in breast cancer using a combined MRI morphological features, radiomics, and deep learning approach based on dynamic contrast-enhanced MRI. J Magn Reson Imaging. 2024; 59: 2238-2249. (PMID: 37855421) **[Crossref]**
32. Martincich L, Deantoni V, Bertotto I, Redana S, Kubatzki F, Sarotto I, et al. Correlations between diffusion-weighted imaging and breast cancer biomarkers. Eur Radiol. 2012; 22: 1519-1528. (PMID: 22411304) **[Crossref]**
33. Park SH, Choi HY, Hahn SY. Correlations between apparent diffusion coefficient values of invasive ductal carcinoma and pathologic factors on diffusion-weighted MRI at 3.0 Tesla. J Magn Reson Imaging. 2015; 41: 175-182. (PMID: 24353241) **[Crossref]**
34. Thakur SB, Durando M, Milans S, Cho GY, Gennaro L, Sutton EJ, et al. Apparent diffusion coefficient in estrogen receptor-positive and lymph node-negative invasive breast cancers at 3.0T DW-MRI: A potential predictor for an oncotype Dx test recurrence score. J Magn Reson Imaging. 2018; 47: 401-409. (PMID: 28640531) **[Crossref]**
35. Durando M, Gennaro L, Cho GY, Giri DD, Gnanasigamani MM, Patil S, et al. Quantitative apparent diffusion coefficient measurement obtained by 3.0Tesla MRI as a potential noninvasive marker of tumor aggressiveness in breast cancer. Eur J Radiol. 2016; 85: 1651-1658. (PMID: 27501902) **[Crossref]**
36. Byon JH, Park YV, Yoon JH, Moon HJ, Kim EK, Kim MJ, et al. Added Value of MRI for invasive breast cancer including the entire axilla for evaluation of high-level or advanced axillary lymph node metastasis in the post-ACOSOG Z0011 trial era. Radiology. 2021; 300: 46-54. (PMID: 33904772) **[Crossref]**
37. Chen H, Meng X, Hao X, Li Q, Tian L, Qiu Y, et al. Correlation Analysis of Pathological Features and Axillary Lymph Node Metastasis in Patients with Invasive Breast Cancer. J Immunol Res. 2022; 2022: 7150304. (PMID: 36249424) **[Crossref]**
38. Kayadibi Y, Kocak B, Ucar N, Akan YN, Yildirim E, Bektas S. MRI radiomics of breast cancer: machine learning-based prediction of lymphovascular invasion status. Acad Radiol. 2022; 29(Suppl 1):S126-S134. (PMID: 34876340) **[Crossref]**